

INFRARED POSITIONING AND COMMUNICATION UNIT FOR A NANOROBOTICS PLATFORM OPERATING IN A COLD HELIUM ATMOSPHERE

Sylvain Martel¹ and Guido Baumann^{1,2}

¹NanoRobotics Laboratory, Computer Engineering Dept., École Polytechnique de Montréal (EPM),
Campus of University of Montréal, Montréal (Québec) Canada

²University of Karlsruhe, Mechanical Engineering Dept., Karlsruhe, Germany

E-mail: sylvain.martel@polymtl.ca

Abstract – The development of a new nanorobotics platform based on a fleet of scientific instruments configured as wireless miniature robots capable of fast operations at the nanoscale in a cooling chamber has been proposed. To cope with the excessive heat of the robots, the heat dissipation is enhanced by filling the chamber with cooled Helium. While the high-powered robots can be maintained at relatively low operating temperatures, the infrared positioning and communication systems needed to coordinate the robots, would without protection, be permanently damaged when exposed to such low ambient temperature levels. This paper describes the design of an infrared and communication unit capable to operate under these excessive conditions while fulfilling the communication and coordination requirements of such a nanorobotics platform.

I. INTRODUCTION

The concept of nanofactories [1] based on a fleet on miniature robots capable of nanometer-scale operations have been proposed and described [2, 3]. One example of such a robot is the NanoWalker [4] as depicted in Fig. 1 and in Fig. 2.

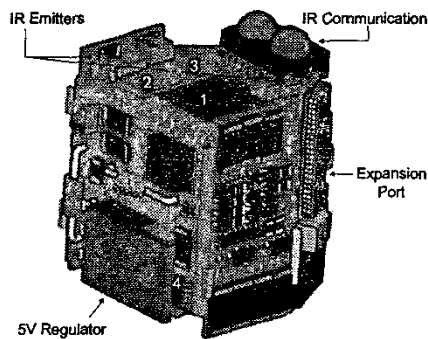


Fig.1. Top view of the NanoWalker robot (from [4])

As shown in the Computer-Aided Design (CAD) models in Fig. 1 and Fig. 2, a fair amount of electronics including an onboard computer indicated by the parts

numbered 1, 2, and 3 in Fig 1, must be embedded onto the 32-mm diameter robot.

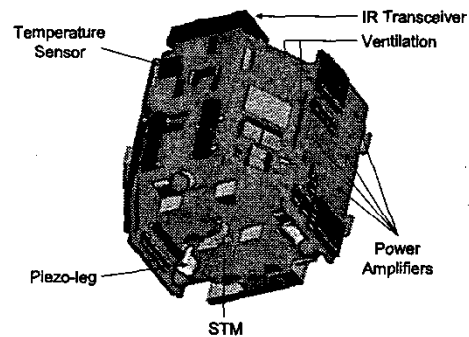


Fig.2. Bottom view of the NanoWalker robot (from [4])

The electronics system, also shown in Fig. 3, provides the required functionality for autonomous and fast Scanning Tunneling Microscope-based (STM) [5] operations at the nanoscale.

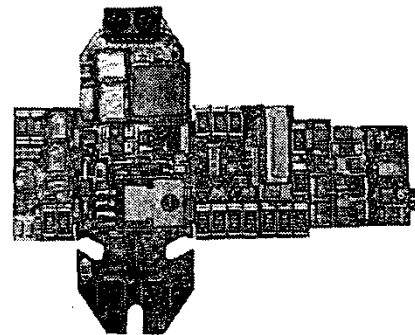


Fig.3. Photograph of the electronics circuit (outer face shown only)

STM has been used not only for imaging but also for other tasks. Nanomanipulation for instance can be performed using an STM. In all existing nanomanipulation systems using STM or other types of Scanning Probe Microscopes (SPM), teleoperation is used in most cases. In a teleoperation system, a human operator

is part of the control-loop and directly performs nanomanipulation through a Human-Machine Interface (HMI) using force-feedbacks [6]. Because one of the main objectives of the proposed nanorobotics platform is high throughput operations, including a human operator in the control-loop is obviously not suitable. A suitable but more ambitious approach is automatic nanomanipulation based on a task-oriented approach using closed-loop automatic control. However, the automatic control at the nanoscale is not reliable at the present time [7]. Nonetheless, with intensive researches, this issue is most likely to be resolved in a relatively near future. In the mean time, other tasks such as high throughput inspections at the nanoscale are feasible with the proposed platform and existing techniques. The other advantages of relying on a fleet of miniature instrumented robots compared to a more conventional instrument architecture, is the added degree of freedom in displacement of the instruments, an increase in density of instruments per surface area, the ease of combining several types of instruments on the same platform, and the flexibility of adding, removing or replacing instruments without restructuring the whole platform. Furthermore, the approach based on wireless miniature instrumented robots, increases the resonant frequency of the instrumentation systems, making it less sensitive to lower frequency vibrations.

Unfortunately, these advantages are paid by a heat dissipation problem due to a significant increase in density of high performance electronics. It is estimated and confirmed with preliminary tests that the embedded electronic system shown in Fig. 3 will dissipate between 15 and 20W of power on average. Other approaches, e.g. [8], avoids this problem by embedding no electronics or only the low powered instrument electronics and related interfaces linked with wires to the high powered electronics located at a remote site. In this case, only a few miniature robots can work on the same platform, limiting the achievable throughput. To avoid wires to be tangled especially with potentially more than 100 of these robots working in an area not exceeding $0.8\text{m} \times 0.8\text{m}$ and because experiments [9] have shown that wires prevent repetitive nanometer-scale displacements of these robots, a wireless implementation was essential in our case. For achieving very high throughput, relying on an external computer for many tasks in order to decrease the power consumption was not an option because of the too large communication latency and response time.

Miniaturization of the robots is also a critical aspect for increasing the flexibility and the throughput of the platform by an increase of the density of instruments per surface area. By doing so, the surface available on each miniature robot to dissipate the heat from the high-

powered embedded electronics becomes insufficient. Adding heat sinks, heat pipes or similar devices is not an option since they would increase substantially the overall size of the robots. Because in our knowledge, no other micro- or nanorobots seem to have similar cooling problems within the constraints imposed by such approach, a novel solution had to be found. As such, to cope with the cooling problem of the miniature robots without increasing significantly their overall size, a cooling chamber, shown in Fig. 4 and Fig 5, has been developed [10]. The transition of liquid Nitrogen to a gas state in a cooling unit shown in Fig. 4 is used to cool Helium gas circulating through a cooling chamber. Helium is being used since it is an inert gas, preventing many problems encountered with air such as oxidation and molecular interactions with the samples. Furthermore, Helium has 4.8 times the heat conductivity of air. The high heat conductivity of the ambient atmosphere allows a significant reduction of the flow during force cooling, leading to a reduction of turbulences caused by neighbored robots. This in turn makes the control of the sensitive instruments at the nanoscale easier through a significant reduction of thermal drifts.

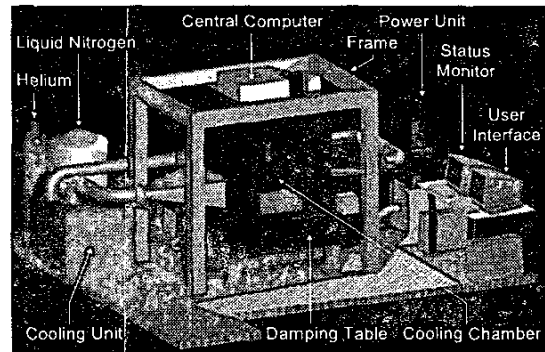


Fig.4. CAD representation of the cooling chamber (from [10])

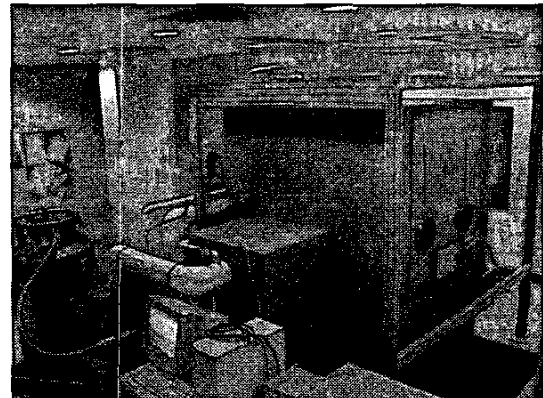


Fig.5. Photograph of the cooling chamber

The temperature of each robot is monitored by three embedded electronic temperature sensors (one is shown in Fig. 2). Two temperature sensors are placed on the outer surface but on opposite faces, and one is placed inside the robot's structure where the STM tip resides. Such configuration provides a good estimation of the temperature distribution of each robot. Typically, the robot's internal operating temperature is allowed to fluctuate between 0 and 70°C. A special thin jacket made of copper with miniature fins and ceramic plates surrounding the robot is used to spread the heat evenly throughout the exposed outer surface. When the internal temperature exceeds an upper or lower pre-programmed threshold, an interrupt signal is sent to the robot's embedded processor. A message is then transmitted by the robot through one of the four 4 Mb/s half-duplex Infrared (IR) communication link to inform a central computer (see Fig. 4). The central computer then interrogates all robots through the same IR communication link to gather an up-to-date overall temperature profile among all robots. Based on the temperature profile but more specifically on the minimum and/or maximum temperature levels, as well as the position of each robot obtained through the IR positioning systems, a specific temperature regulation algorithm is applied.

II. OPTICAL AND ELECTRONIC SYSTEMS

Fig. 6 shows inside the cooling chamber. As depicted in Fig. 6, four Position or Photo Sensing Detection (PSD) unit and IR communication transceivers are used for global positioning [11] and wireless communication.

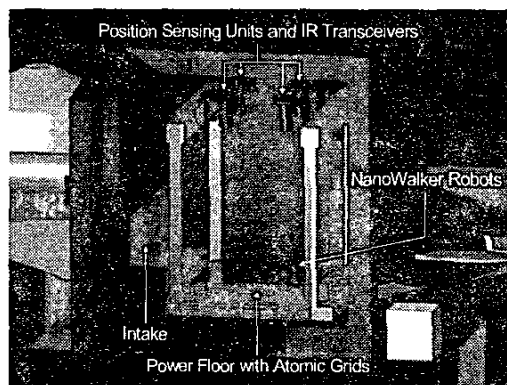


Fig.6. View inside the cooling chamber (from [10])

The PSD units based on a 2-D lateral effect photodiode provide resolutions in positioning down to a few micrometers. The present design uses a 4.0/45 mm lens in front of the PSD to provide working cells with a diameter of 330 mm, leading to a lens to IR emitter (on top of each

robot) distance of 777.58 mm. This distance also dictates the height of the chamber since no obstructions or even glasses causing distortions could be put in the line of sight of the sensitive PSD system. These specifications also take into account the emitting angle of 24° of the IR emitters. Two IR emitters on the top of each robot (see Fig. 1) are used to determine the planar and angular positions of each robot.

With the present implementation, past experiments have shown that 90 dB (15 bits) of positioning resolution can be easily achieved every 10 μs, and some further improvements, especially in the presence of white Gaussian noises, can be achieved through a longer integration time. For a planar operating cell of 330 mm in diameter, these figures yield a high speed positioning resolution of ~10μm. Atomic-scale positioning is achieved by "counting" atoms with the embedded STM tip on special atomic grids made of Highly Oriented Pyrolytic Graphite (HOPG) embedded onto a "powerfloor" [12] (see Fig. 2). The link between the STM-based and the PSD-based positioning systems are done through a special reference patterns engraved on the HOPG grids using a Focus Ion Beam (FIB) [13]. In order to support a fleet exceeding 100 NanoWalker robots for achieving up to 20×10^6 STM-based measurements/s per platform, four IR positioning and communication units operating in the 875-nm wavelengths are implemented.

III. THERMAL ENCLOSURE

Although in most cases, ambient temperature levels of approximately -60°C are expected, the lowest temperature level that can be reached with the cooling chamber depicted in Fig. 5 when filled with Helium gas is -185°C. It becomes obvious that at such low temperature levels, a protective enclosure is needed for both the optical and electronics systems required for global positioning and communication. The design of thermal enclosure of the IR positioning and communication unit is depicted in Fig. 7. To provide good accessibility, the enclosure is divided in two parts. One top part, the "roof", is fixed to the frame depicted in Fig. 6. The frame inside the cooling chamber is attached to the edge of the powerfloor and it is conceived to have a resonant frequency as close as possible to the high resonant frequency of the robots. An additional damping system is installed underneath the powerfloor to filter excessive high frequency vibrations.

The lower part referred to as the cap is removable, even after the installation of the whole enclosure. This is necessary for certain tasks, especially in an experimental setting that may require further adjustments of the PSD lens for instance. Closing of the enclosure is facilitated by a guidance fixed on the roof and screws joining the cap

and tightened from below. All systems are mounted in a line, parallel to the door of the cooling chamber, to ensure good accessibility. The design uses four different materials and all threads are tapped into metal plates to facilitate the assembly by superseding bolts. The walls for the enclosure are assembled using two thin plates as inner and outer walls. The hollow space in between is filled with an insulating material.

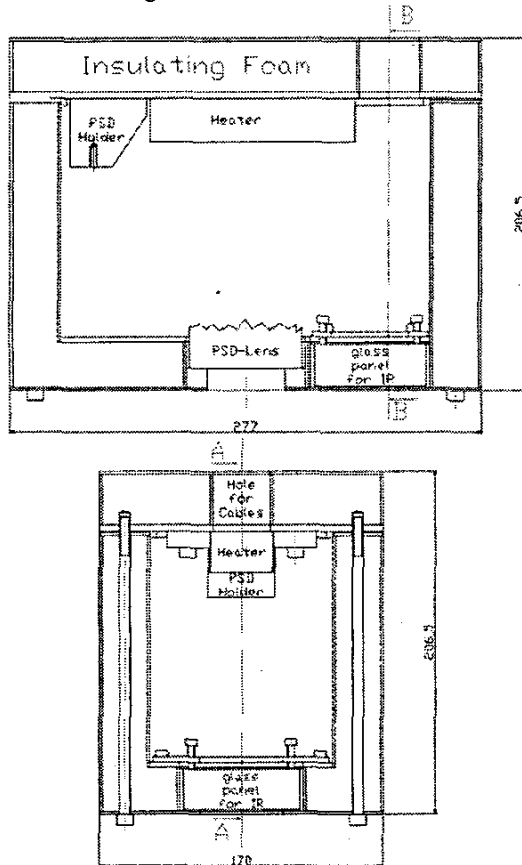


Fig. 7. Drawings of the thermal enclosure (scale in mm)

Stainless steel was chosen as the material for the walls. Stainless steel is relatively rigid allowing relatively thin panels (1.5 mm) to be mounted. This in turn allows the size of the enclosure to be reduced or the space for the insulation to be increased, or a combination of both within the space constraints of the platform. Stainless steel has also a lower coefficient of thermal expansion ($\alpha = 16 \times 10^{-6} \text{ }^\circ\text{K}^{-1}$) and thermal conductivity ($\lambda = 16 \text{ W/(m }^\circ\text{K)}$) compared to other conventional materials such as aluminum for instance with $\alpha = 25 \times 10^{-6} \text{ }^\circ\text{K}^{-1}$ and $\lambda = 150 \text{ W/(m }^\circ\text{K)}$. Furthermore, stainless steel does not oxidize and the joints can be easily welded, and threads can be

tapped to have removable junctions. The minimum size of the enclosure is mainly defined by the necessary space for the PSD and the IR communication sub-systems. Additionally, cables, connectors, and a heater must also fit into the same enclosure. The PSD and the IR transceiver are mounted on the roof in an adjustable way supported by slotted holes so that their position can be modified in the x-, y-, and z-axis. The PSD is also mounted on a z-stage (from Opto Sigma) to allow accurate adjustment in the z-axis. As depicted in Fig. 7, the PSD lens with an optical filter are directly exposed through an opening to the cold ambient atmosphere without protecting glass as in the case for the IR transceiver in order to avoid distortions that would affect significantly the resolution of the PSD system. This opening has a slightly larger diameter than the diameter of the lens. A circular gasket closes the gap providing room for thermal expansion and allowing rotation of the lens during adjustment of the focal point. Although distortion is also a concern for the IR communication link, it is significantly less critical than in the case of the PSD unit. Nonetheless, a special glass (BOROFLOAT® 33 Borosilicate Float Glass from Schott) with a very little absorption of IR light (very high IR transparency), a low thermal expansion, a low thermal conductivity, with superior surface finish and flatness, was selected. The diameter of the glass has been selected to guarantee no obstruction to the $\pm 15^\circ$ of line of sight of the IR communication path.

IV. THERMAL INSULATION

An effective thermal insulation for the positioning and communication unit is a critical issue in such an environment. The heat exchange between the chamber and the heated interior of the enclosure should be as low as possible and as such, the choice of the insulation material is of prime concern. Polyurethane (thermal conductivity of $0.017 \text{ W/(m }^\circ\text{K)}$) has been selected as a material of choice for this particular application since it is available in high-density foam, which ensures a 100% filling of the entire steel panel structure of the unit. The heat dissipation through the walls of the enclosure can be estimated with the Fourier law (Eq. 1).

$$\dot{Q} = -\lambda \cdot A \cdot \frac{d\vartheta}{dx} \quad (1)$$

In Eq. 1, for the dissipated heat in Watts [W], λ is the thermal conductivity [$\text{W/(m}^\circ\text{K)}$] and A is the surface area [m^2]. For a flat wall, Eq. 1 becomes:

$$\dot{Q} = -\lambda \cdot A \cdot \frac{\Delta\vartheta}{\Delta x} = -\lambda \cdot A \cdot \frac{\vartheta_2 - \vartheta_1}{\Delta x} \quad (2)$$

V. THERMAL IMPACT ON THE LENS

In Eq. 2, $\Delta\vartheta$ is the difference in temperature inside and outside the enclosure in Kelvin [$^{\circ}\text{K}$] and Δx is the wall thickness [m]. A trade-off has to be found regarding the size of the enclosure and the thickness of the insulation within the space constraints of the platform. After several iterations, 30 mm was selected as the wall thickness of the enclosure (2×1.5 mm for the stainless steel inner and outer walls and 27 mm of insulating foam). For the final estimations, the average surface area of the enclosure was taken into account, i.e. the average of the surface areas of the inner and the outer walls. For the calculations, an arbitrary target temperature of 20°C (approximately mid-point in the 0 - 50°C range to guarantee proper operations of all systems) was chosen inside the enclosure, and -120°C (between the lowest and average temperature inside the chamber) as the temperature in the cooling chamber. By substituting the dimensions of the enclosure A in Eq. 2 is written as:

$$A = 2 \cdot (w_1 \cdot h_1 + h_2 \cdot d_1 + w_2 \cdot d_2). \quad (3)$$

In Eq. 3, $w_1 = 0.247$ m, $h_1 = 0.173$ m, $d_1 = 0.14$ m, $w_2 = 0.247$ m, and $d_2 = 0.14$ m. With the the specifications and substituting Eq. 3, Eq. 2 is computed as:

$$\dot{Q} = -0.017 \frac{\text{W}}{\text{m} \cdot \text{K}} \cdot A \cdot \frac{20^{\circ}\text{C} - (-120^{\circ}\text{C})}{0.027 \text{ m}} = -17.9 \text{ W} \quad (4)$$

The result of Eq. 4 gives the heat loss by conduction through the walls of the enclosure and calculated for the ideal case, i.e. a completely sealed enclosure with homogenous material. It can be assumed that practically, the heat loss may slightly be higher due to some factors such as the gaps filled by gaskets, which provide less insulating performance compared to other sections entirely filled with the insulating foam.

To compensate for the thermal loss of the enclosure, a heater with a heat emission higher than 17.9W needs to be embedded in the enclosure. A 20W DC heater to minimize Electro-Magnetic Interferences (EMI) to be fixed to the roof within the enclosure was selected. The heat is controlled by varying the DC voltage level instead of relying on simpler techniques such as on-off control which could cause significant electrical interferences and couplings to the sensitive embedded positioning system. The temperature within the enclosure is measured by a thermocouple mounted on the PSD, since it is the most sensitive instrument to thermal variations. The temperature is typically maintained by the heater to within $\pm 2.5^{\circ}\text{K}$ (set accordingly to an acceptable positioning error of the PSD specified at a worst case level of 200 ppm/ $^{\circ}\text{K}$) of an arbitrary set point.

To avoid optical distortions, the optical filter and the front of the lens attached to the PSD unit are directly exposed to the low ambient temperature of the cooling chamber. As such, special considerations had to be taken into account.

The lens and filter (from Schneider Optics) are guaranteed to work correctly from -20°C to $+55^{\circ}\text{C}$ typically. Although the filter can tolerate temperature levels beyond these values, the lens is more sensitive and the focus may change substantially beyond these values. The climatic and environmental audits for these optical units were done previously by the company Schneider Kreuznach according to the standard ISO 9022 (DIN 58390). These tests cover a temperature range between -25°C and 70°C . We estimate that beyond those values, when directly exposed to an ambient temperature of approximately -100°C for instance, the clearance of the diaphragm should remain constant and the lens should not create image distortions. The putty of the lens is thermally resistant down to a temperature of -125°C . Since the glass transition temperature of the glue used for the lens is about -40°C , it is possible that further cooling could not be compensated any more, and therefore permanent damages to the glued joints could occur. The diameter fits of the lens seats decrease by approximately 30 μm compared to the diameter of the lens. As the clearances of the fits are smaller, the lens mountings (aluminum or brass) shrink on the lens and could potentially crush or damage it. The lens mountings shrink approximately 15 μm in the axial direction relative to the case or packaging of the lens. Hence, L-shaped elastic threaded rings are used to hold the lens and to compensate for such changes in dimensions. Nonetheless, the change in ambient temperature is always done as slow as possible to avoid thermal shocks. Furthermore, the index of refraction of the lens depends strongly on the temperature. As such, warming bands glued on the lens are also considered to minimize thermal impacts. For the shrinking of the lens-mount on the lens, there are two aspects to consider: First, the thermal conductivity of the lens glass ($\lambda_{\text{glass}} < 1 \text{ W}/(\text{m} \cdot \text{K})$) is much smaller than the thermal conductivity of the aluminum lens mounting ($\lambda_{\text{aluminum}} > 116 \text{ W}/(\text{m} \cdot \text{K})$; $\lambda_{\text{brass}} > 115 \text{ W}/(\text{m} \cdot \text{K})$). Therefore, the temperature of the lens casing follows much more quickly the ambient temperature inside the cooling chamber. This effect can be eliminated by changing the temperature very slowly at the cost of extended latencies in regulating the ambient temperature in the chamber, adding constraints in maintaining the temperature of all robots with minimum variations causing possible thermal drifts on the sensitive instruments. Second, the coefficients of thermal

expansion of the lens mounting material ($\alpha_{\text{aluminum}} = 2.3 \times 10^{-5} \text{ } ^\circ\text{K}^{-1}$; $\alpha_{\text{brass}} = 2.0 \times 10^{-5} \text{ } ^\circ\text{K}^{-1}$) and of the lens ($\alpha_{\text{glass}} = 0.9 \times 10^{-5} \text{ } ^\circ\text{K}^{-1}$) are very different and this phenomenon can be reduced by minimizing temperature changes. Since the temperature of the cooling chamber is driven by the need of cooling the robots within specific temperature constraints, one solution to consider is to heat also the sections of the lens that are exposed to the ambient temperature by using a warming band.

To avoid condensation caused by humidity during the cooling cycle, a purging system connected to the cooling chamber purged with Helium is also embedded in the enclosure. The purging system is provided by two small tubes, one entering and one exiting, conducting the Helium from the gas bottle beside the nanorobotics platform through the top part of the cooling chamber into the enclosure.

VI. SUMMARY

This paper gave an overview of the main technical issues related to the design of a thermal enclosure for a special IR position and communication unit used for the coordination of a fleet of approximately 100 miniature robots capable of nanoscale operations through an embedded STM. As the size of these instrumented robots decreases to increase the density of instruments per surface area, while the throughput of each robot increases, heat dissipation due to a reduction of the surface area per robot available to dissipate the heat becomes problematic and cannot be solved with known traditional techniques. One proposed technique is the use of a cooled Helium atmosphere in a special cooling chamber to increase heat transfer while decreasing the flow during force cooling in order to minimize thermal drifts that could affect the resolution of the instruments. In order to maintain the temperature of each robot within an operational range, the Helium atmosphere must be cooled well below the operating level of electronics and optical systems that must reside in the same chamber. As such, a thermal enclosure becomes essential to maintain these systems in an operational state.

The fabrication of such enclosure was made as flexible as possible with the size adjusted to the constraints of the nanorobotics platform including the angles of sight of the PSD and IR communication transceivers and emitters. Stainless steel and Polyurethane have been used to build the enclosure. 27 mm of thermal insulation using Polyurethane foam and a 20W heater embedded in the enclosure was used to provide sufficient protection for the optical and electronic systems.

ACKNOWLEDGEMENT

This project is funded by the Canada Research Chair (CRC) in Conception, Fabrication and Validation of Micro/Nanosystems and the National Sciences and Engineering Research Council of Canada (NSERC).

REFERENCES

- [1] J. Breguet, C. Schmitt, and R. Clavel, "Micro/nanofactory: Concept and state of the art," *Proc. of SPIE: Microrobotics and Microassembly*, Vol. 4194, pp. 1-12, Nov. 2000.
- [2] S. Martel and I. Hunter, "Nanofactories based on a fleet of scientific instruments configured as miniature autonomous robots," *Proc. of the 3rd Int. Workshop on Microfactories (IWMF)*, pp.97-100, Sept. 2002
- [3] S. Martel, S. Riebel, T. Koker, M. Sherwood, and I. Hunter, "Large-scale nanorobotic factory automation based on the NanoWalker technology," *Proc. of the 8th IEEE Int. Conf. on Emerging Technologies and Factory Automation, Special Session on Microrobotics in Manufacturing*, Oct. 2001
- [4] S. Martel, L. Cervera Olague, J. Bautista Coves Ferrando, S. Riebel, Koker T., J. Suurkivi, T. Fofonoff, M. Sherwood, R. Dyer, and I. Hunter, "General description of the wireless miniature NanoWalker robot designed for atomic-scale operations," *Proc. of SPIE: Microrobotics and Microassembly*, Vol. 4568, pp. 231-240, Oct. 2001
- [5] C.J. Chen, "Introduction to scanning tunneling microscope," *Oxford University Press*, New York, 412 pages, 1993
- [6] R.L. Hollis, S. Salcudean, and D.W. Abraham, "Toward a tele-nanorobotic manipulation system with atomic scale force feedback and motion resolution," *Proc. of the IEEE Int. Conf. on MEMS*, pp. 115-119, 1990
- [7] M. Sitti and H. Hashimoto, "Teleoperated nano scale object manipulation," *Recent Advances on Mechatronics*, pp. 322-335, ed. By O. Kaynak, S. Tosunoglu and M.J. Ang, Springer Verlag Pub., Singapore, 1999
- [8] S. Fatikow, St. Fahlbusch, St. Garnica, H. Hülsen, A. Kortschack, A. Shirinov, and A. Sill, "Development of a versatile nanohandling station in a scanning electron microscope," *Proc. of the 3. Int. Workshop on Microfactories (IWMF)*, pp. 31-34, Sept. 2002
- [9] S. Martel, A. Saraswat, A. Michel, and I. Hunter, "Preliminary evaluation and experimentation of the push-slip method for achieving micrometer and sub-micrometer step sizes with a miniature piezo-actuated three-legged robot operating under high normal forces," *Proc. of SPIE: Microrobotics and Microassembly*, Vol. 4194, pp. 141-148, Nov. 2000
- [10] S. Martel, A. Schindler, G. Baumann, S. Riebel, and T. Boitani, "Cooling platform for an automated nano-factory based on a fleet of miniature robots designed for atomic scale operations", *Proc. of IEEE Automation*, May 2003
- [11] S. Martel, O. Roushdy, M. Sherwood, and I. Hunter, "Optical high resolution positioning system for miniature robot," *Proc. of SPIE: Microrobotics and Microassembly*, Vol. 4194, pp. 121-128, Nov. 2000
- [12] S. Martel S., W. Garcia de Quevedo, and I. Hunter, "Techniques for continuous power delivery to a group of 15-Watt +3.3 to ±150 VDC miniature wireless instrumented and fast stepping robots through several thousand intermittent contacts per second between the robots' legs and the walking surface," *Proc. of SPIE: Microrobotics and Microassembly*, Vol. 4194, pp. 168-177, Nov. 2000
- [13] D. St.-Jacques, S. Martel, and T. Boitani, "Nanoscale grid based positioning system for miniature instrumented robots," *Proc. of the Canadian Conf. on Electrical and Computer Eng. (CCECE)*, May 2003